Robust detection of heart beats in multimodal records using slope- and peak-sensitive band-pass filters

2015 Physiol. Meas. 36 1645

(http://iopscience.iop.org/0967-3334/36/8/1645)

IOP Publishing | Institute of Physics and Engineering in Medicine Physiological Measurement

Physiol. Meas. **36** (2015) 1645–1664 doi:10.1088/0967-3334/36/8/1645

Robust detection of heart beats in multimodal records using slope- and peak-sensitive band-pass filters

Urška Pangerc and Franc Jager

Faculty of Computer and Information Science, University of Ljubljana, Večna pot 113, 1000 Ljubljana, Slovenia

E-mail: franc.jager@fri.uni-lj.si

Received 27 February 2015
Accepted for publication 3 June 2015
Published 28 July 2015

Abstract

In this work, we present the development, architecture and evaluation of a new and robust heart beat detector in multimodal records. The detector uses electrocardiogram (ECG) signals, and/or pulsatile (*P*) signals, such as: blood pressure, artery blood pressure and pulmonary artery pressure, if present. The base approach behind the architecture of the detector is collecting signal energy (differentiating and low-pass filtering, squaring, integrating). To calculate the detection and noise functions, simple and fast slope- and peak-sensitive band-pass digital filters were designed. By using morphological smoothing, the detection functions were further improved and noise intervals were estimated. The detector looks for possible pacemaker heart rate patterns and repairs the ECG signals and detection functions. Heart beats are detected in each of the ECG and *P* signals in two steps: a repetitive learning phase and a follow-up detecting phase. The detected heart beat positions from the ECG signals are merged into a single stream of detected ECG heart beat positions. The merged ECG heart beat positions and detected heart beat positions from the *P* signals are verified for their regularity regarding the expected heart rate. The detected heart beat positions of a *P* signal with the best match to the merged ECG heart beat positions are selected for mapping into the noise and no-signal intervals of the record. The overall evaluation scores in terms of average sensitivity and positive predictive values obtained on databases that are freely available on the Physionet website were as follows: the MIT–BIH Arrhythmia database (99.91%), the MGH/MF Waveform database (95.14%), the augmented training set of the follow-up phase of the PhysioNet/Computing in Cardiology Challenge 2014 (97.67%), and the Challenge test set (93.64%).

Keywords: robust heart beat detection, multimodal records, slope- and peak-sensitive band-pass filters, detecting pacemaker pattern, bedside monitors

(Some figures may appear in colour only in the online journal)

1. Introduction

Continuous long-term multimodal records obtained from bedside monitors and other devices that record electrocardiogram (ECG) and other physiological signals, such as pulsatile signals, provide important information about the status of cardiac activity. There is an increasing need for robust and efficient automatic heart beat detection, which is also the most important and basic step in further processing such as heart beat classification and arrhythmia analysis, or estimating ST segment level for each detected heart beat and detecting transient ischaemia.

The problem of accurate automatic detection of heart beats is older then computer science and is still not sufficiently solved. Many excellent heart beat detectors have been developed (Pahlm and Sörnmo 1984, Pan and Tompkins 1985, Köhler *et al* 2002, Elgendi *et al* 2014, Oweis and Al-Tabbaa 2014). These heart beat detectors rely on ECG signals only and are based on detecting QRS complexes of ECGs. There is still a lack of robust and accurate heart beat detectors in noisy data. Usually, the QRS complex detectors consist of a preprocessing phase where they try to eliminate noise and emphasize QRS complexes, but often the signals are just too noisy or even lost.

The idea of the PhysioNet/Computing in Cardiology Challenge 2014 (the Challenge) (Moody *et al* 2014) was to develop robust multi-channel heart beat detectors that also rely on other simultaneous physiological signals. These multimodal signals include a variety of pulsatile signals (*P* signals) such as blood pressure (BP), arterial blood pressure (ABP), and pulmonary artery pressure (PAP). The participants in the Challenge were asked to developed robust heart beat detectors using multimodal data, which meant discovering relationships between the ECG signal and other available physiological signals in order to improve the accuracy of detecting heart beats. Most of the teams' solutions (De Cooman *et al* 2014, Ding *et al* 2014a, Ghosh *et al* 2014, Gierałtowski *et al* 2014, Gilián *et al* 2014, Johannesen *et al* 2014, Johnson *et al* 2014, Pangerc and Jager 2014, Plešinger *et al* 2014, Pimentel *et al* 2014, Schulte *et al* 2014, Vollmer 2014, Yang *et al* 2014, Yu *et al* 2014) relied on *P* signals, which are closely related to cardiac activity.

This paper presents the development, architecture, and evaluation of a robust, fast, efficient, gain-independent, multimodal data heart beat detector, based on slope- and peak-sensitive band-pass filters, which is an improved version of a previously developed heart beat detector (Pangerc and Jager 2014) for the Challenge.

2. Methods

2.1. Development and test databases

The proposed detector was developed and evaluated using the MIT–BIH Arrhythmia database (Moody and Mark 2001), the Long-Term ST (LTST) database (Jager *et al* 2003), the MIT–BIH Polysomnographic database (Ichimaru and Moody 1999), the Massachusetts General Hospital/Marquette Foundation Waveform (MGH/MF) database (Welch *et al* 1991), and the augmented training and test sets of the follow-up phase of the Challenge, which ended at the end of February 2015. All these databases are freely available on the Physionet website (Goldberger *et al* 2000). The MIT–BIH Arrhythmia database contains 48 two-channel

half hour ECG records sampled at 360 samples per second. The LTST database contains 86 two- and three-channel 24 h ECG records sampled at 250 samples per second. The MIT–BIH Polysomnographic database contains 18 multi-channel records with one ECG channel and other multiparameter channels (with one BP channel) of length from 1.17 to 6.3 h sampled at 250 samples per second. The MGH/MF Waveform database contains 250 multi-channel records with three ECG channels and other channels such as BP, ABP and PAP channels of length from 18 to 86 min sampled 360 samples per second. The *augmented training set* (200 records) and the *test set* (200 records) of the follow-up phase of the Challenge comprise records of length of 10 min with one ECG channel, and BP, ABP and PAP channels. The *augmented training set* (200 records) is composed from the *old training set* (100 records sampled at 250 samples per second) that was available prior to the follow-up phase and from the *new training set* comprised of 100 records (10 records sampled at 250 samples per second and 90 records sampled at 360 samples per second) that was added to the *old training set* during the follow-up phase.

2.2. Detector overview

The development strategy behind the proposed detector is to analyze ECG signals as accurately as possible, to estimate noise intervals in the ECG signals, and after that to map the positions of the detected heart beats in the selected *P* signal into the noise intervals and intervals with ECG signal loss. The basic approach for detecting signal regions with the most prominent features (slopes and peaks of QRS complexes, steep slopes of the systolic pressure) that define the positions of heart beats is differentiating and low-pass filtering the signals, squaring (collecting signal energy), and further integrating (Pan and Tompkins 1985).

Figure 1 shows a block diagram of the proposed heart beat detector, *repdet*. The detector deals with up to three simultaneous ECG signals and/or up to three simultaneous *P* signals in a record, such as BP, ABP or PAP. The algorithms *recg* and *rpls*, and the *matching procedure* of the detector can be summarized as follows:

1. *Preprocessing*. The algorithms *recg* and *rpls* derive the ECG and *P* detection functions, and the ECG noise functions, using simple integer–multiplier band-pass digital filters (Lynn 1977). The *recg* algorithm initially looks for a pacemaker heart rate pattern, which is a new feature of the proposed detector over our previous detector (Pangerc and Jager 2014), and repairs intervals of ECG signals and detection functions that contain pacemaker pulses. The ECG and *P* detection functions are further improved by using the morphological smoothing algorithm (Gonzalez and Woods 2008).
2. *Detection step I (repetitive learning phase)*. Both algorithms, *recg* and *rpls*, detect heart beats in each of the ECG and *P* signals, and noise intervals are estimated in each of the ECG signals. The detected heart beats in this phase have to pass strict rules. Therefore, these detected heart beats in the ECG or *P* signals are considered as true and accurate. The detected heart beat positions in an ECG or *P* signal are refered to as the ECG or *P* signal *heart beat annotation stream*.
3. *Merging ECG heart beat annotation streams*. The ECG heart beat annotation streams of the repetitive learning phase are merged together into one single heart beat annotation stream from all ECG signals and an ECG signal containing the shortest duration of noise intervals is selected for detection step II.
4. *Detection step II*. In this follow-up detection phase, both algorithms, *recg* and *rpls*, look for the remaining heart beats in the signals. If no *P* signals are present, the ECG heart beat annotation stream of the *recg* algorithm is considered as final.

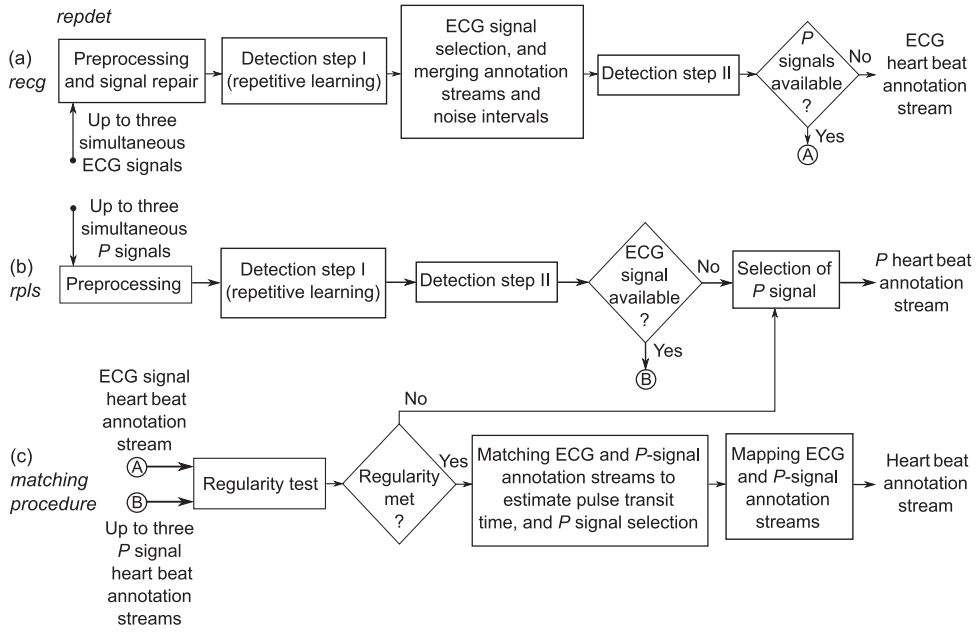

Figure 1. Block diagram of the proposed detector, *repdet*. (a) The algorithm *recg* that detects heart beats in the ECG signals. (b) The algorithm *rpls* that detects heart beats in the *P* signals. (c) The matching procedure that merges the detected heart beat positions (annotations) from the ECG and *P* signals into one single heart beat annotation stream.

5. *Selection of P signal*. If no ECG signals are present, the *rpls* algorithm selects a *P* signal of which the number of totally detected heart beats is closer to the expected number of heart beats for the record, and its annotation stream is considered as final.
6. *Regularity test*. A regularity test, a new feature of the proposed detector over our previous detector (Pangerc and Jager 2014), between the annotation streams of detected heart beats in the ECG and *P* signals, verifies the expected average heart rates of the ECG and *P* signals. If regularity is not met, the detector conveys the heart beat annotation stream of the selected *P* signal by the *rpls* algorithm as final.
7. *Matching ECG and P signal annotation streams*. A matching process between the ECG and *P* signal annotation streams, estimates the pulse transit times between the QRS complexes and pulses of the *P* signals. A *P* signal annotation stream with the highest matching index is selected for the final step of mapping the positions of detected heart beats into one single heart beat annotation stream.
8. *Mapping P signal annotation stream*. Heart beat annotations of the selected *P* signal are mapped into noise intervals of the record and its longer intervals with no detected heart beats.

2.3. Preprocessing

2.3.1. Feature extraction. With the aim of deriving the ECG and *P* detection functions, a class of simple and fast integer-multiplier digital filters was used (Lynn 1977). We designed a slope-sensitive, $H_{E1}(z)$, and a peak-sensitive, $H_{E2}(z)$, sampling-frequency adjustable band-pass filters, which extract peaks and slopes of QRS complexes, with the following transfer functions:

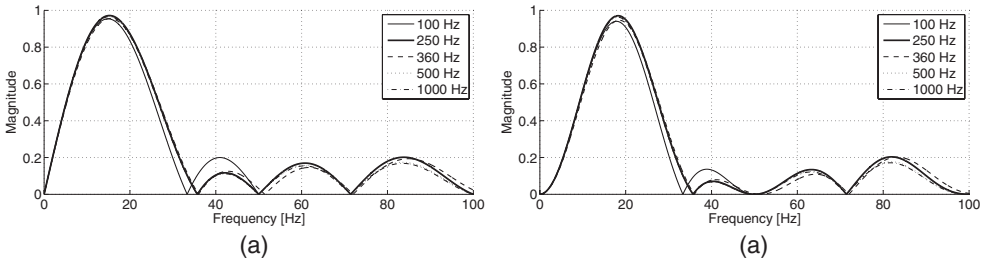

Figure 2. The transfer functions of the filters (1) for a variety of sampling frequencies (F_S) of 100 Hz, 250 Hz, 360 Hz, 500 Hz, and 1000 Hz. The functions are plotted up to the $F_S/2$. (a) The QRS slope-sensitive filter, $H_{E1}(z)$. (b) The QRS peak-sensitive filter, $H_{E2}(z)$.

$$H_{E\,m}(z) = (1 - z^{\lfloor -5 \cdot F_S/F_{S_0} \rceil})^m \cdot \frac{(1 - z^{\lfloor -7 \cdot F_S/F_{S_0} \rceil})}{(1 - z^{-1})}, m = 1, 2, \tag{1}$$

where $\lfloor . \rceil$ denotes rounding of the argument, F_S is the sampling frequency of the input signals, and $F_{S_0} = 250$ Hz is the reference sampling frequency. The first term in (1) is the first or the second-order differentiator, while the second term is the low-pass moving average filter. By rounding the exponents of the transfer functions, the filters become sampling-frequency adjustable.

In figure 2, the transfer functions of the filters H_{E1} and H_{E2} for variety of typical sampling frequencies in a multimodal data environment are shown. It is possible to simply resample signals in a multimodal data environment, however the chosen class of filters is easy to modify with respect to sampling frequency, while keeping the desired frequency bands and their integer coefficients. The filters have desired pass-bands of approximately 10–24 Hz. This is the frequency band from which QRS complexes are mainly composed (Thakor *et al* 1984). The filters are much less sensitive to the ECG P- and T-waves, which comprise lower frequencies. Both filters attenuate low frequencies (<10 Hz), which may also be high due to baseline wander and motion artefacts, and high frequencies (>24 Hz), which may be high due to power line interference, random noise and muscle noise.

The impulse responses of the filters $H_{E1}(z)$ and $H_{E2}(z)$, in the case of $F_S = 250$ samples per second, are as follows:

$$h_1 = (1, 1, 1, 1, 1, 0, 0, -1, -1, -1, -1, -1), \tag{2}$$

$$h_2 = (1, 1, 1, 1, 1, -1, -1, -2, -2, -2, -1, -1, 1, 1, 1, 1, 1). \tag{3}$$

Their lengths are 48 ms and 68 ms, which are approximate durations of the slopes and peaks of a normal QRS complex. The impulse responses (2) and (3) show characteristics of the first and second derivation while attenuating higher unwanted frequencies. The filters (1) are non-recursive with the finite impulse responses and simple coefficients, and are computationally inexpensive.

It would be possible to use standard finite impulse response filters such as wavelets or Mexican hat (Laplacian of Gaussian—LoG) impulse response with real number coefficients (but higher computation complexity) to extract slopes and peaks of QRS complexes. The architecture of the LoG filter (which would extract peaks) is the Gaussian low-pass filter followed by the second-order differentiator, or vice versa, since both processes are linear. Similarly, it would be possible to use the Gaussian low-pass filter followed by the first-order

differentiator to extract slopes. In our robust approach, we used the first- and second-order differentiator followed by the moving average low-pass filter. The difference between the two approaches is in using the moving average low-pass filter instead of the Gaussian low-pass filter. If we compare the transfer functions of the two filters, significant differences appear only in the stop-band. The Gaussian filter shows a continuously decreasing frequency characteristic, while the moving average filter ripple and zeros. Since the higher frequencies are unwanted in our case, and are additionally attenuated by further squaring and integrating, in order to derive efficient detection functions, the approach using moving average low-pass filter is suitable and yields sufficient filtering results.

We implemented the $H_{E1}(z)$ and $H_{E2}(z)$ filters even more efficiently, i.e. recursively with only a few additions per signal sample. In the case of $F_S = 250$ samples per second the difference equations of the filters $H_{E1}(z)$ and $H_{E2}(z)$ are as follows:

$$y_1(i) = y_1(i-1) + x(i) - x(i-5) - x(i-7) + x(i-12), \tag{4}$$

$$y_2(i) = y_2(i-1) + x(i) - 2x(i-5) - x(i-7) + x(i-10) + 2x(i-12) - x(i-17), \tag{5}$$

where $x(i)$ and $y(i)$ denote input and output signal samples. Since the poles of the transfer functions are cancelled by zeros, the filters remain stable and with a linear phase characteristic.

To derive the ECG noise detection functions, we similarly designed a slope-sensitive, $H_{N1}(z)$, and a peak-sensitive, $H_{N2}(z)$, band-pass filter with the pass-bands approximately 24–56 Hz:

$$H_{N\,m}(z) = (1 - z^{\lfloor -3 \cdot F_S/F_{S_0} \rceil})^m, \quad m = 1, 2. \tag{6}$$

These two filters (6) are sensitive to high frequency noises, boundaries of random shifts, as well as QRS complexes. Note that the QRS complex is a region with sharp peaks and slopes, and is also comprises higher frequencies above 24 Hz.

To extract significant slopes of the *P* signals, especially the first steep slope region of the systolic pressure intervals, which are the most significant features of the *P* signals, we designed a slope-sensitive band-pass filter, $H_P(z)$, with the following transfer function:

$$H_P(z) = (1 - z^{\lfloor -25 \cdot F_S/F_{S_0} \rceil}) \cdot \frac{(1 - z^{\lfloor -50 \cdot F_S/F_{S_0} \rceil})}{(1 - z^{-1})}. \tag{7}$$

The filter has a step-shape impulse response, considered as an approximation to the steep slope segments of the *P* signals, and desired pass-band 1.2–3.5 Hz. This is the frequency band from which a steep slope segment of the first anacrotic wave, in the *P* signals is expected to be composed.

2.3.2. Detection functions. The initial ECG detection function, $e_1(i)$, of each ECG signal, where i denotes original signal sample number, is derived following:

$$e_1(i) = L_E((|y_{E1}(i - (D_{E2} - D_{E1}))| + |y_{E2}(i)|)^2), \tag{8}$$

where y_{E1} and y_{E2} are the outputs of the filters H_{E1} and H_{E2}, D_{E1} and D_{E2} are their corresponding delays, and $L_E(.)$ denotes further smoothing using a sampling-frequency adjustable low-pass moving average filter. The use of two filters and summing the absolute values of their outputs assures that the detected function pulses are dense and single also for wider QRS complexes of abnormal heart beats. Since the typical shape of a QRS complex is a sequence of peaks and slopes, the use of, e.g. a slope sensitive filter only, may result in two detection pulses per wide abnormal beats and thus false detections. By squaring (collecting signal

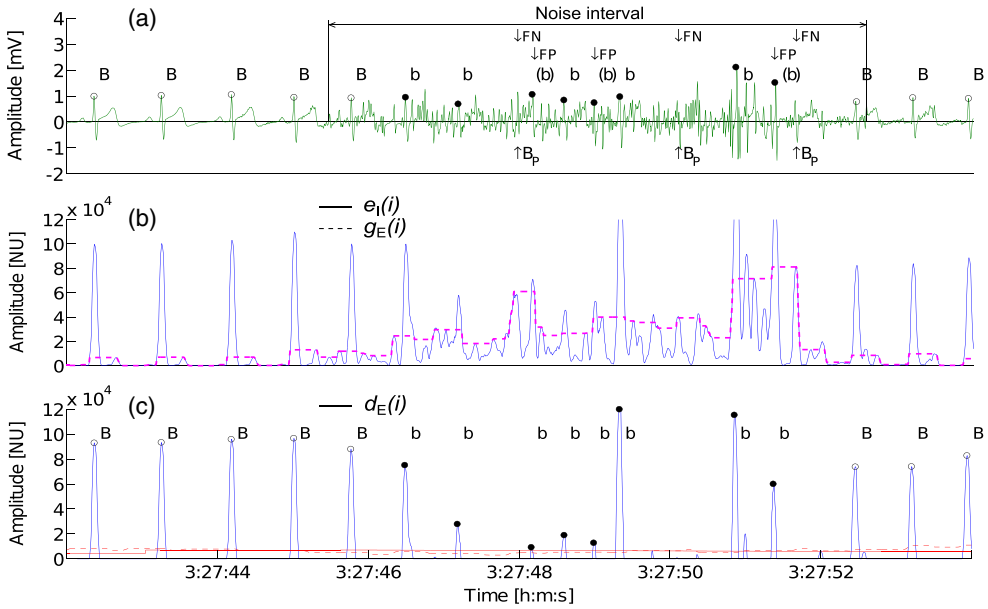

Figure 3. Deriving the ECG detection functions in part of record slp03 from the MIT–BIH Polysomnographic database. (a) Original ECG signal; (b) initial ECG detection function, $e_I(i)$, and its morphologically smoothed version, $g_E(i)$; (c) the final ECG detection function, $d_E(i)$, and detection thresholds of the detection step I, $T_{E1}(i)$, (dashed line), and II, $T_{E2}(i)$ (solid line); upper case B and B_p (and circles) and lower case b (and dots) mark heart beats detected in steps I, and II, respectively. *FP*—false positive detections, (b)—falsely detected and rejected heart beats, *FN*—false negative detections, B_p—inserted heart beat annotations from the *P* signal of the record into the noise interval.

energy), autocorrelation of the spectum is performed thus increasing the desired frequency components. The cut-off frequency of the low-pass moving average filter, which additionally attenuates high frequencies, is approximately 6.5 Hz. An example of the initial ECG detection function, $e_I(i)$, is shown in figure 3.

The ECG noise function, $n_E(i)$, of each ECG signal (see figure 4), is derived as follows:

$$n_E(i) = L_N((|y_{N1}(i - (D_{N2} - D_{N1}))| + |y_{N2}(i)|)^2), \tag{9}$$

where y_{N1} and y_{N2} are the outputs of the filters H_{N1} and H_{N2}, D_{N1} and D_{N2} are their corresponding delays, and $L_N(.)$ denotes further smoothing using a sampling-frequency adjustable low-pass moving average filter with a cut-off frequency of approximately 16 Hz.

The initial *P* detection function, $p_I(i)$, of each *P* signal, is derived as follows:

$$p_I(i) = \begin{cases} y_P^2(i) \text{ if } & y_P(i) > 0, \\ 0 & \text{otherwise}, \end{cases} \tag{10}$$

where y_P is the output of the filter H_P (see figure 5). Squaring of the *P* detection function is an improved feature of the proposed detector over our previous detector (Pangerc and Jager 2014). If detection pulses of detection functions are produced by squaring, and if decision rules to detect pulses are based on peak amplitude criteria of the detection pulses, similar amplitudes of the detection pulses are more likely to correspond to similar heart beat shapes

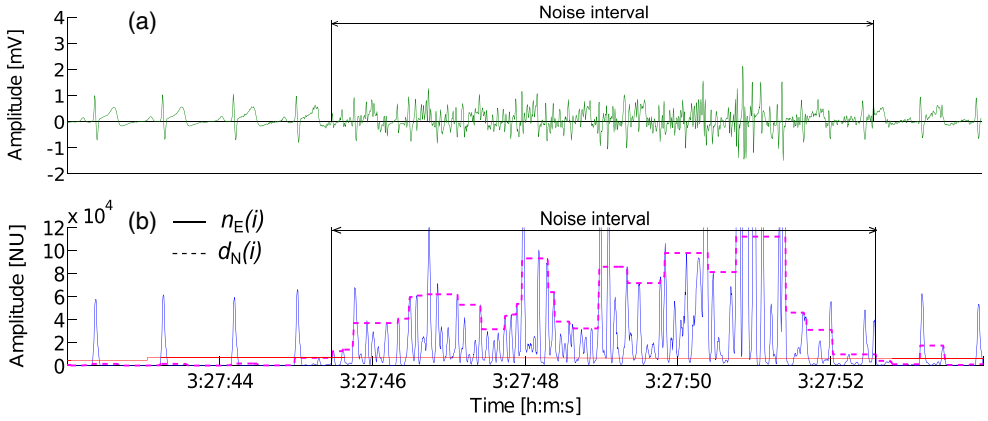

Figure 4. Deriving the ECG noise detection function in part of record slp03 from the MIT–BIH Polysomnographic database. (a) Original ECG signal; (b) the ECG noise function, $n_E(i)$, and the ECG noise detection function, $d_N(i)$, with marked noise interval, and the threshold, $T_{E_2}(i)$ (solid line).

of the signals, which is important when strictly searching for consecutive sequences of similar heart beats.

2.3.3. Morphological analysis. Morphological algorithms are already used for the task of detecting QRS complexes (Chen and Duan 2006, Zhang and Lian 2009). Morphological smoothing of a function f is defined by morphological *opening* followed by *closing* using a structuring element b. *Opening* of a function f by a structuring element b is $f \circ b = (f \ominus b) \oplus b$ where $\ominus$ denotes *erosion* of the f by the element b,

$$(f \ominus b)(i) = \min_{n \in b}\{f(i+n)\}, \tag{11}$$

and $\oplus$ denotes *dilation* of the f by the element b,

$$(f \oplus b)(i) = \max_{n \in b}\{f(i+n)\}. \tag{12}$$

Closing of the function f by the structuring element b is $f \bullet b = (f \oplus b) \ominus b$.

In this work, we used morphological smoothing to further improve the shape of the ECG and *P* detection functions, and to derive the ECG noise detection function. The structuring element in our case is simply a sliding window within which minimum or maximum is searched for. The final ECG detection function, $d_E(i)$, is composed using the following rule:

$$d_E(i) = \begin{cases} e_I(i) - g_E(i) & \text{if} \quad e_I(i) - g_E(i) \geqslant 0, \\ 0 & \text{otherwise}, \end{cases} \tag{13}$$

where $g_E(i)$ is the morphologically smoothed version of $e_I(i)$, with the structural element of length of 220 ms. Morphological smoothing and subtracting reject various fluctuations and bumps at the base of the initial detection function due to noise, and ECG P- and T-waves, while leaving the shape of the QRS detection pulses unchanged (see figure 3). Morphological smoothing of the ECG noise function, $n_E(i)$, using a structuring element of 300 ms, produces the ECG noise detection function, $d_N(i)$, which is a smooth stepwise envelope over the peaks of the ECG noise function, $n_E(i)$, in the noise intervals (see figure 4). Morphological smoothing fills the gaps within these noise intervals and rejects unwanted spikes left in the QRS

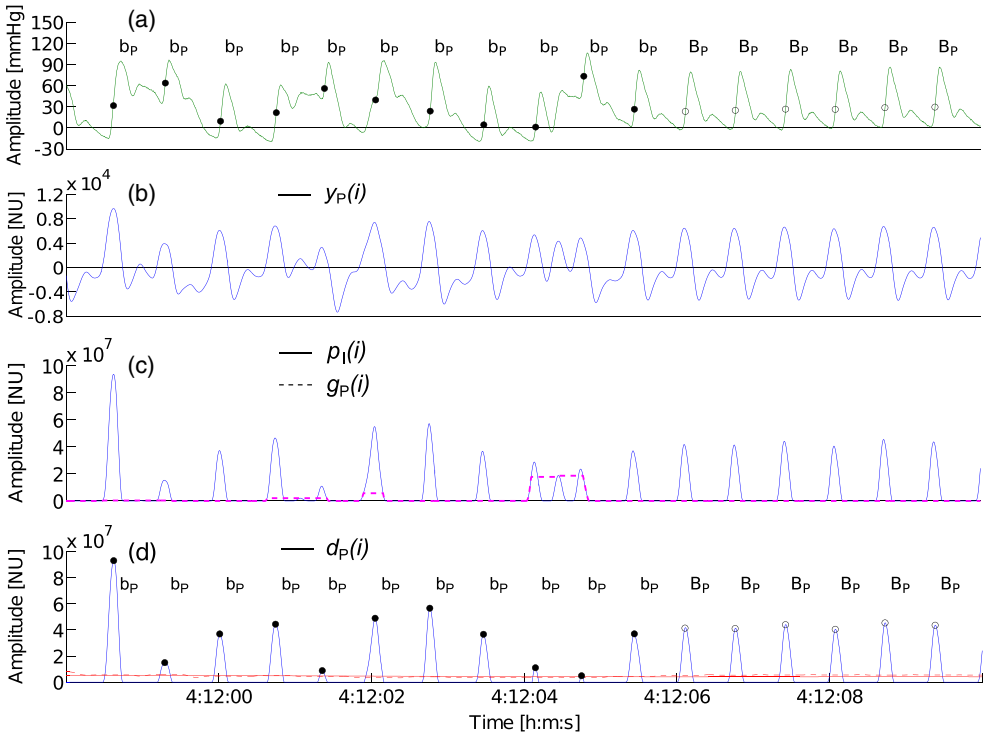

Figure 5. Deriving the *P* detection functions in part of record slp03 from the MIT–BIH Polysomnographic database. (a) Original *P* signal (BP) of the record; (b) filtered ECG signal using $H_P(z)$; (c) initial *P* detection function, $p_I(i)$, and its morphologically smoothed version, $g_P(i)$; (d) the final *P* detection function, $d_P(i)$, with detection thresholds from the detection step I, $T_{P1}(i)$ (dashed line), and II, $T_{P2}(i)$ (solid line). Upper case B_p (and circles) and lower case b_p (and dots) mark heart beats detected in detection steps I, and II, respectively.

complex intervals outside these noise intervals. The final *P* detection function, $d_P(i)$, is composed using the same rule, with a structuring element of 300 ms in length. The $g_P(i)$, which is the morphologically smoothed version of the initial *P* detection function, $p_I(i)$, is conditionally subtracted from the $p_I(i)$. A trace of a heart beat in the *P* signals is a steep slope followed by two waves, the first and higher anacrotic wave, and the second and smaller dicrotic wave. By using a morphological smoothing approach, higher positive peaks of the $d_P(i)$ are kept, while lower positive peaks due to possible noise or isovolumetric relaxation period fluctuations are suppressed (see figure 5).

The lengths of the structuring elements were initially estimated according to the nature of waves due to physiological differences of the ECG and *P* signals. The length of 220 ms to process ECG signals was tuned and validated using the MIT–BIH Arrhythmia database, while the length of 300 ms was used to derive the ECG noise detection function and to process the *P* signals, using the MGH/MF Waveform database and the new training set of the follow-up phase. The criteria was approximately an equal overall number of false negative, *FN*, and false positive, *FP*, detections.

2.3.4. Signal repair. For the purpose of ECG signal repair due to a pacemaker, a routine of the *recg* algorithm initially searches for a pacemaker pattern. A typical pacemaker pattern is

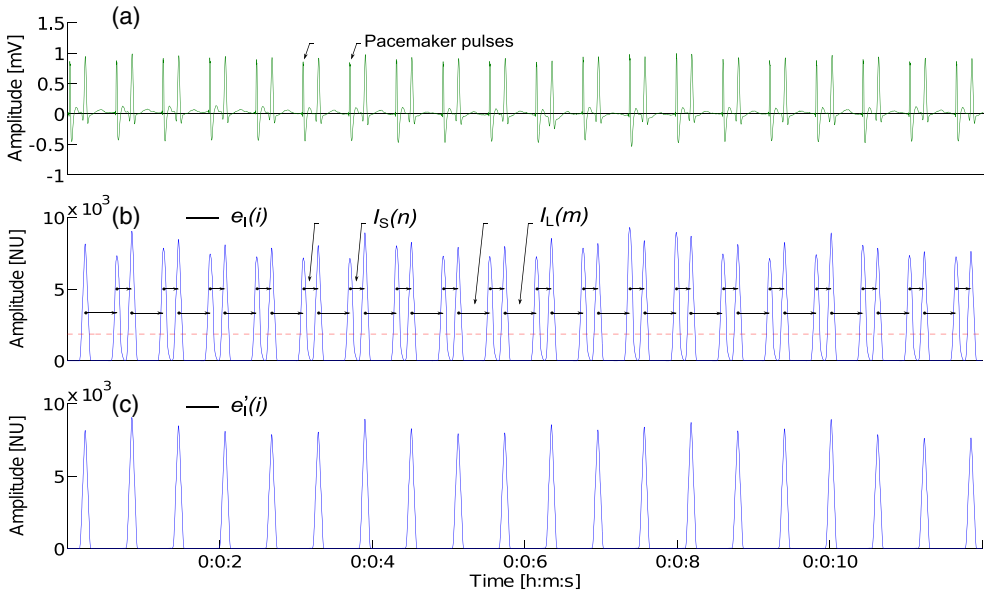

Figure 6. Detecting pacemaker pattern and signal repair in record 41173 of the new training set. (a) Original ECG signal of the record with pacemaker; (b) initial ECG detection function, $e_I(i)$, with marked shorter, $I_S(n)$, and longer, $I_L(m)$, beat-by-beat intervals of initially detected heart beats, and detection threshold, T_{E0} (dashed line); (c) repaired initial ECG detection function, $e_I'(i)$.

shown in figure 6. Each QRS complex of ECG signal is preceded by a pacemaker pulse which may typically be monophasic or biphasic. The routine roughly detects heart beats in the initial ECG detection function, $e_I(i)$, using the threshold T_{E0} calculated as a median of the running moving average of the $e_I(i)$ within a 4 s window. The pacemaker pattern is recognized if a high double-class regularity of the beat-by-beat intervals of detected pulses in the $e_I(i)$ is met. if the total number of detected heart beats does not differ for more than $\pm$25% from the expected number of detections according to the length of the record and the average beat-by-beat interval, and if the average beat-by-beat interval of detected heart beats is less than 410 ms, the detected heart beats are grouped into two sets, the first, $I_S(n)$, with shorter (<95%) and the second, $I_L(m)$, with longer (>105%) beat-by-beat intervals according to the average beat-by-beat interval. A pacemaker pattern is considered to be present if the total number of heart beats in these two sets is more than 75% of all detected heart beats, and if the ratio of numbers of heart beats in both sets does not differ by more than 25%. In this case, 200 ms signal intervals of ECG signal and initial ECG detection function, $e_I(i)$, that correspond to detected heart beats from the set one are cut out yielding a repaired initial ECG detection function, $e_I'(i)$. The routine was designed empirically on the basis of examples from the new training set and from the MGH/MF Waveform database.

2.4. Detection step I (repetitive learning phase)

In this step, the algorithm *recg* repetitively seeks for as many four similar consecutive pulses in each final ECG detection function, $d_E(i)$, as it can find them throughout the record (Pangerc and Jager 2014). To accept and mark four consecutive pulses as heart beats, the following conditions have to be satisfied:

1. differences of the time intervals between the four pulses are less than 20%;
2. differences of the amplitudes between the four pulses are less than 30%;
3. the time intervals between the four pulses have to be longer than 300 ms (heart rate of 200 bpm) and less than 1.7 s (heart rate of 35 bpm).

The detection threshold, $T_{E1}(i)$, is set as a moving average within a 4 s window of the final ECG detection function, $d_E(i)$. After detecting each of the four pulses, the algorithm starts to look for the next such four pulses, while the last pulse of the previous four pulses becomes the first tentative pulse of the next such four pulses. Each such of four detected pulses is marked as valid heart beats (see figure 3, the detected heart beats are marked as B). Detection step I is actually a repetitive learning phase, since each next four detected heart beats do not rely on any information about previously detected heart beats. The purpose of this approach is to detect sequences of very similar, normal, and final heart beats, likely out of noise intervals (see figure 3). The rule of four beats also offers that the detected heart beats are out of rhythm abnormalities, the only exception is ventricular tachycardia.

After each four similar consecutive pulses, the trace of the detection threshold for the detection step II, $T_{E2}(i)$, is derived. (The threshold $T_{E2}(i)$ is also used for detecting noise intervals.) It is calculated as the mean value of the ECG noise function, $n_E(i)$ (see figure 4), of the corresponding four heart beats, multiplied by 1.3, and is linearly interpolated between each of the next four pulses found. Since the threshold $T_{E2}(i)$ is derived from the ECG noise function, $n_E(i)$, high frequencies of the corresponding QRS complexes efficiently estimate a reasonably low threshold for the follow-up detection step II. In addition, the average value of intervals between the four pulses defines the ECG heart rate for these four heart beats, $\bar{h}_E(j)$, in beats per minute, where j denotes the ECG heart beat number. The ECG heart rate, $\bar{h}_E(j)$, is linearly interpolated between each of the next four pulses found as well.

Noise intervals are detected in the ECG noise detection function, $d_N(i)$ (see figure 4). Any segment where the $d_N(i)$ exceeds the threshold, $T_{E2}(i)$, for a time longer then 0.5 s, is marked as a noise interval.

A similar repetitive four-beat learning approach is applied to each final P detection function, $d_P(i)$, by the algorithm *rpls* yielding an annotation stream of detected P signal pulses (see figure 5; the detected heart beats are marked as B_p). The detection threshold, $T_{P1}(i)$, is set as a moving average within a four-second window of the final P detection function, $d_P(i)$. This time, the detection threshold for step II, $T_{P2}(i)$, is calculated directly from the final P detection function, $d_P(i)$, and is multiplied by 0.75. The interpolated detection threshold, $T_{P2}(i)$, and the interpolated P pulse rate, $\bar{p}_P(k)$, in pulses per minute [ppm], where k denotes P signal heart beat number, are also calculated.

Considering the thresholds $T_{E1}(i)$ and $T_{P1}(i)$ of detection step I, an alternative approach using a moving median within a 4 s window of the final ECG and P detection functions, yielded practically equal performances of the developed detector using all of the development databases of this study.

2.5. Merging ECG heart beat annotation streams

The algorithm *recg* merges the ECG heart beat annotation streams as detected separately in each of simultaneous ECG signals during detection step I. For this purpose, it uses a 300 ms sliding tolerance window to avoid possible reference point mismatch and duplication of the same heart beat positions found in simultaneous ECG signals. It means that the detected heart beat positions from simultaneous ECG signals which are less then 300 ms apart are merged into one single heart beat position into the center of sliding tolerance window. The algorithm

also selects the ECG signal containing the shortest duration of noise intervals and additionally rejects or shortens its noise intervals with respect to the heart beat positions detected in other simultaneous ECG signals. Note that at this step, the algorithm deals with heart beat positions detected after the repetitive learning phase, which are likely to be out of noise intervals. The final ECG detection function, $d_E(i)$, and the detection threshold, $T_{E2}(i)$, of the selected ECG signal, are inputs to detection step II.

2.6. Detection step II

In this follow-up detection phase, both algorithms *recg* and *rpls* seek for the rest of QRS complexes and *P* signal pulses that correspond to heart beats, using interpolated thresholds $T_{E2}(i)$ and $T_{P2}(i)$. Refer to figures 3 and 5, the detected heart beats are marked as b and b_p, respectively. The constants 1.3 and 0.75, by which the two thresholds are multiplied, were determined by the criteria of approximately equal number of false negative, *FN*, and false positive, *FP*, detections using the MIT–BIH Arrhythmia and MGH/MF Waveform databases, and the new training set of the follow-up phase.

2.7. Selection of P signal

If no ECG signal is present, or if the regularity test between the annotation streams from the ECG and *P* signals fails, the *rpls* algorithm selects one of the *P* signal annotation streams as final. The selected *P* signal annotation stream is that of which number of detected pulses is closer to the expected number of pulses for the record according to the duration of the record and its average pulse rate $\bar{p}_P$. The reference points of the heart beats are corrected for the estimated default average pulse transit time, PTT_D. The PTT_D was estimated using the new training set and is 140 ms. The optimization criteria was the highest overall performance of the developed detector obtained on the new training set.

2.8. Regularity test

The routine to seek for pacemaker pattern fails if a high double-class regularity of the beat-by-beat intervals of the detected pulses in the initial ECG detection function, $e_I(i)$, is not obtained. This happens in the case where the pacemaker—QRS and QRS—pacemaker intervals are approximately equal. Therefore, at this step, the regularity test verifies the validity of the rates of the ECG and *P* signal annotation streams. If the average heart rate of the ECG signal, $\bar{h}_E$, is approximately two times higher than the average pulse rate, $\bar{p}_P$, of any *P* signal, $0.75 < 2 \cdot \bar{h}_E/\bar{p}_P < 1.25$, than the pacemaker is likely to be present, and the detector switches to *P* signals only.

2.9. Matching ECG and P signal annotation streams

In order to allow the heart beat annotation stream of a *P* signal to be mapped into the annotation stream of the ECG signal, matching between the annotation streams needs to be performed. Matching is applied between the ECG annotation stream and each of the *P* signal annotation streams. The purpose of matching is to estimate the average pulse transit time (*PTT*) between the QRS complexes and the steep slope intervals of the *P* signal. The matching method used is the correlation between the annotation streams of the detected heart beats. The entire annotation stream of the *P* signal is sample-by-sample shifted versus the annotation

stream of the ECG signal for all those heart beats of the ECG signal that were detected outside noise intervals. The correlation window is of duration of $[0.10 \cdot 60/\bar{h}_E, 0.50 \cdot 60/\bar{h}_E]$ seconds, where $\bar{h}_E$ denotes the average heart rate of the ECG signal. A number of matching heart beats in the ECG and *P* signal is calculated according to the matching window of length of ± 140 ms which is put onto each heart beat position of the *P* signal annotation stream, and at each sample-by-sample shift. The shift with the highest number of matching heart beats defines the average *PTT* for the *P* signal. During the matching, a matching index, *M*, is determined for each of the *P* signals too. It is defined as the number of matching heart beat pairs in the ECG and *P* signal versus the number of heart beats detected in the ECG signal but outside noise intervals. The *P* signal annotation stream of the *P* signal with the highest *M* is then selected by using the matching procedure for the mapping routine. If its *M* is higher than 0.75, the selected *P* signal annotation stream is also marked as 'accurate'.

2.10. Mapping the P signal annotation stream

Heart beat annotations of the selected *P* signal are finally mapped into the noise intervals of the ECG signal and its longer intervals with none of the detected heart beats. Within each noise interval, the detector first searches for heart beats detected in the *P* signal. For each such *k*th heart beat from the *P* signal, the detector then searches back for heart beats in the ECG-signal annotation stream in the mapping window of duration of $[-0.14 \cdot 60/\bar{h}_P(k), +0.14 \cdot 60/\bar{h}_P(k)]$ seconds, shifted for the duration of the estimated average *PTT* where $\bar{h}_P(k)$ is the interpolated *P* pulse rate for the *k*th heart beat. If the *P* signal was previously marked as 'accurate' according to the matching index, the pulse transit time is previously determined average pulse transit time, *PTT*, otherwise the pulse transit time is the default average pulse transit time, PTT_D. The heart beat that is closest to the center of the mapping window is confirmed as final. If there are no heart beats in the mapping window, the *k*th heart beat annotation from the *P* signal is mapped into the ECG-signal annotation stream at the center of the mapping window. An example of mapping *P* signal annotations into a noise interval of the ECG signal is shown in figure 3. The rest of heart beats within the noise intervals are rejected, unless they were detected in detection step I, or they had a mapping pair. Mapping of heart beats from the *P* signal is also performed for ECG signal intervals with none of the detected heart beats which are due to missed heart beats or signal loss. Such gaps are defined as intervals that are longer than 1.6 times the interpolated ECG heart rate, $60/\bar{h}_E(j)$.

2.11. Performance metrics and sample detectors

The detector developed in this work was evaluated using the following performance measures: gross and average sensitivity (*Se*) defined as $TP/(TP + FN)$, and gross and average positive predictive value (*PPV*) defined as $TP/(TP + FP)$, where *TP* is the number of true positive detections, *FN* is the number of false negative detections, and *FP* is the number of false positive detections. Furthermore, we define the overall score, *S*, given performance trial, or the Challenge entry, as the average of these four statistics, gross and average *Se*, and gross and average *PPV*. The performances obtained in this study on the development databases were calculated using the standard freely available beat-by-beat annotation comparator *bxb* (Moody *et al* 1993, Goldberger *et al* 2000) with the option of no learning phase. Further details of the performance metrics, performance measures, gross and average statistics, overall score given performance trial or entry, as well as of the annotation comparator *bxb*, can be found in Silva *et al* (2015).

Table 1. Heart beat detection performance comparison using the MIT–BIH Arrhythmia database.

	MIT–BIH A			Gross	
Algorithm	Beats	*FN*	*FP*	*Se*(%)	*PPV*(%)
Pan and Tompkins (1985)	109809	277	507	99.75	99.54
Hamilton and Tompkins (1986)	109267	340	248	99.69	99.77
Li *et al* (1995)	104182	112	65	99.89	99.94
Martínez *et al* (2004)	109428	220	153	99.80	99.86
Ghaffari *et al* (2008)	110159	120	322	99.91	99.72
Adnan *et al* (2009)	109494	253	393	99.77	99.64
Elgendi (2013)	109985	247	124	99.78	99.87
Ding *et al* (2014b)	109494	73	134	99.93	99.88
recg[a]	109494	125	125	99.89	99.89
recg	109494	114	92	99.90	99.92

[a] Only the first ECG signal of the records was processed.

Performances of the detector *repdet*, and algorithms *recg* and *rpls*, developed in this study, were compared to the *gqrs* heart beat detector (Moody *et al* 2014, Silva *et al* 2015, Physionet 2014a), that was the sample entry during 2014 challenge, and to the *wabp* algorithm (Zong *et al* 2003, Physionet 2014b) to detect arterial blood pressure pulses.

2.12. Assessing robustness

Robust methods for parameter extraction and data fusion for use in intensive case units are becoming important (Clifford *et al* 2009). As the spirit of the Challenge was the robust detection of heart beats in multimodal data, we also evaluated the proposed detector in the sense of robustness. To assess the robustness of the detector we used the bootstrap estimation of performance distribution method (Efron 1979). This method assumes that the database used for the bootstrap is a well-chosen representative subset of the population of examples for a given problem domain. The method determines if the performance of a detector is critically dependent on the choice of the database used for testing, and estimates what would be the expected performance of the detector in the real world. The average performance distributions predict performance on a randomly chosen record. Narrower distribution indicates more a robust detector, meaning that such a detector, no matter which records are tested, gives nearly the same performance.

3. Results

3.1. Assessing performance of the proposed heart beat detector

The proposed detector in this work, *repdet*, is capable of detecting heart beats using ECG signals only (algorithm *recg*), using *P* signals only (algorithm *rpls*), or using combination of the ECG and *P* signals. The proposed detector was implemented in the C programming language.

We evaluated the performance of the *recg* algorithm individually using all records of the MIT–BIH Arrhythmia database (see table 1). The results obtained are quite comparable to performances of some other past and recently published algorithms. The performance of the

Table 2. Performance comparison of ECG and *P* signal heart beat detection algorithms.

	LTST				
	Gross		Average		
Algorithm	*Se*(%)	*PPV*(%)	*Se*(%)	*PPV*(%)	*S*(%)
recg	99.98	99.76	99.98	99.74	99.87
MIT–BIH P					
wabp	99.31	99.74	99.26	99.77	99.52
rpls	99.39	99.79	99.33	99.82	99.58
MGH/MF W					
gqrs	87.25	93.97	88.16	92.19	90.39
repdet	96.53	94.11	95.96	93.95	95.14

Table 3. Performance of the proposed heart beat detector obtained on the old and new training sets, and test set, of the Challenge.

	Old & new training set		New training set		Test set[a]		Test set	
repdet	*Se*(%)	*PPV*(%)	*Se*(%)	*PPV*(%)	*Se*(%)	*PPV*(%)	*Se*(%)	*PPV*(%)
Gross	98.10	97.54	96.38	95.35	91.60	89.55	95.65	93.48
Average	97.84	97.21	95.70	94.47	89.23	88.32	93.86	91.57
S(%)	97.67		95.48		89.67		**93.64**	

[a] Only ECG signals.

recg algorithm was also assessed using the entire LTST database (see table 2). Individual evaluation and performance comparison of the *rpls* algorithm to the *wabp* algorithm to detect arterial blood pressure pulses using the entire MIT–BIH Polysomnographic database is also summarized in table 2. For this comparison, the *rpls* algorithm processed one *P* signal per record only (BP) of the database. The default average pulse transit time of 200 ms was used in this particular case, since the *wabp* algorithm was originally evaluated using the average pulse transit time of 200 ms. Moreover, table 2 summarizes performances obtained using the proposed heart beat detector, *repdet*, and the *gqrs* detector that was the sample entry during the Challenge on the entire MGH/MF Waveform database.

Table 3 summarizes the performances obtained for the proposed heart beat detector using the old and new training sets, and test set, of the follow-up phase of the Challenge. The highest scores obtained with the detector presented in this work were 97.67% (old and new training set), 95.48% (new training set) and 93.64% (test set).

Of special iterest are performances of the routine to detect pacemaker heart rate pattern, and of the routine to perform the regularity test, which switches to analysis of *P* signals only in the case of presence of pacemaker. There are 12 records with a pacemaker in the new training set and 20 records with a pacemaker in the MGH/MF Waveform database. In the new training set, five of the pacemakers were detected by the routine to detect a pacemaker pattern in the ECG signal, five were detected by the routine performing the regularity test, while the amplitudes of pacemaker pulses in two records were too low to be detected, or they did not affected the performance. There were no false positive detections of a pacemaker pattern in this set. An example of a successfully detected pacemaker pattern is shown in figure 6. The *Se* and *PPV* in detecting heart beats rose from 64.36% and 77.74%, to 100.00% and 100.00%, respectively, for this record. In the MGH/MF Waveform database, four of the pacemakers were detected

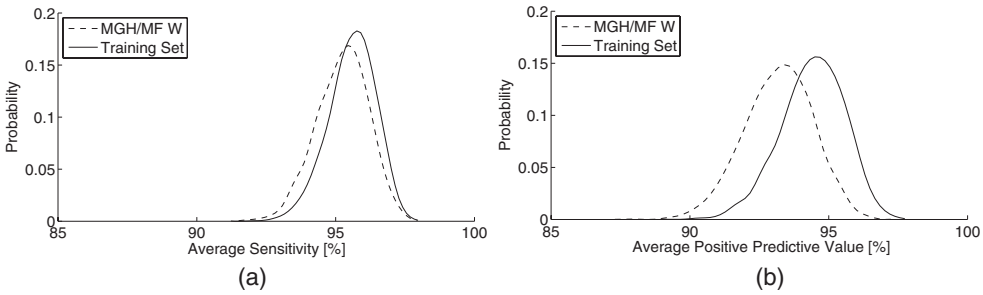

Figure 7. Bootstrap performance distributions of the proposed detector. (a) Average *Se* distributions. (b) Average *PPV* distributions.

Table 4. Statistics of the average *Se* and *PPV* performance distributions.

	Se(%)		*PPV*(%)	
	MGH/MF	New training set	MGH/MF	New training set
Mean	95.24	95.58	93.18	94.41
5% confidence limits	93.66	94.15	91.12	92.49
95% confidence intervals	3.75	3.41	4.91	4.58

by the routine to detect pacemaker patterns, while the amplitudes of pacemaker pulses in the other 16 records were too low to be detected in the selected ECG signal, or they did not affected the performance. In this database, the regularity test failed for two records, but in both records this was due to severe noises in the *P* signals. The rest of development databases of this study do not contain any record with a pacemaker pattern. The two routines to detect pacemaker patterns and to perform the regularity test never caused false positive detections in any of these databases.

3.2. Assessing robustness of the proposed heart beat detector

As the base databases for the bootstrap procedure we used the MGH/MF Waveform database (250 records), and the new training set (100 records) of the follow-up phase, and performed 10 000 bootstrap trials for each database. The average *Se* and average *PPV* performance distributions are shown in figure 7. The detector is less robust for the *PPV* (wider distribution). The robustness of the detector was estimated in the sense of mean performance, the 5% confidence limits (estimating the lowest expected performance in the real world), and with 95% confidence intervals. The results are summarized in table 4. The performance distributions show a lower mean expected *PPV*, a lower expected *PPV* in the real world (5% confidence limits), and wider 95% confidence intervals, if being evaluated using the MGH/MF Waveform database.

4. Discussion and conclusions

In this paper we presented an improved version of our previous robust multimodal data heart beat detector (Pangerc and Jager 2014).

The impulse responses (2) and (3) and the impulse response of the filter (7) may be considered as an approximation to templates for template matching carried out by the matched

filters. In our case the impulse responses would be an approximation to the slopes and peaks of the QRS complex, and to the steep slopes of the *P* signals. One may find a similarity of (3) to the Mexican hat (Laplacian of Gaussian—LoG) convolution kernel of which shapes approximate the shape of the QRS complex waveform (Behar *et al* 2014). One may also find a similarity of the impulse response (3) to a variety of wavelet functions used for the task of QRS complex detection, such as the Dyadic wavelet (Martínez *et al* 2004), or the Mexican hat mother wavelet (Romero *et al* 2005), and even the match of the impulse response (2) to the Haar wavelet (Ghaffari *et al* 2008). One may seek for a better match of an impulse response to the QRS shape using a Gaussian-based convolution kernel with a continuously decreasing frequency characteristic at higher frequencies, however, in our case the Gaussian filter is replaced by a moving average low-pass filter. Using this approach, we obtained sufficient filtering results, and the filters are computationally inexpensive. In addition, the detection functions are squared and low-pass filtered. These two procedures additionally attenuate unwanted high frequencies.

The best scores of our previously developed multimodal heart beat detector (Pangerc and Jager 2014) during phases I, II, and III of the Challenge were 89.24% (second place), 85.91% (third place), and 85.13% (sixth place). Evaluation of the detector with the highest score from phase III in the new scoring environment of the follow-up phase (Silva *et al* 2015) revealed that the time out and zero score occurred for at least one record. In these cases, the execution of the program in the new scoring environment was stopped at that point. There was a function of the code of the detector that became extremely time consuming in the specific noisy signal data segments. After optimizing the code of that function (but keeping the same architecture of the detector), the scores obtained on the new training set (100 records) and on the test set (200 records) of the follow-up phase were 85.38% and 87.34% (entry three), respectively.

The highest score obtained on the test set of the follow-up phase of the Challenge using the detector presented in this work (entry 20) was 93.64%. Inclusion of the *P* signals improved the overall performance of heart beat detection, especially in the ECG noise intervals, where the possibility of false positive detections is high, and in the intervals with ECG signal loss. If we also analyze the *P* signals next to the ECG signals, the overall score of detecting heart beats in the test set rise by 3.97%, i.e. from 89.67% to 93.64% (see table 3).

For the bootstrap procedure to assess the expected performance in the real world, the necessary assumption is that the base database provides a representative set of examples, given the problem domain. In our case, if using the MGH/MF Waveform database as the base database (250 records) for the bootstrap, the expected performances (average *Se* of 93.66% and average *PPV* of 91.12%, see table 4) are close to the actual performances obtained on a (new and unknown) test set of 200 records (average *Se* of 93.86% and *PPV* of 91.57%, see table 3). If using the new training set as the base database (100 records) for the bootstrap, the expected performances (average *Se* of 94.15% and average *PPV* of 92.49%, see table 4) slightly overestimate the actual performances obtained on a (new and unknown) test set of 200 records (average *Se* of 93.86% and *PPV* of 91.57%, see table 3). The proposed detector shows a dependency on the choice of the database, which does not seem to be critical according to small differences of the statistics. The results also indicate that the performance estimates are likely to be optimistic.

Real-time implementation of the detector is possible. There are some limitations regarding decision delay. Considering processing of one ECG signal and *P* signals simultaneously, and excluding the routine to look for pacemaker patterns, a slight modification of the repetitive learning routine and follow-up detecting routine, and excluding the matching procedure of the detector, the overall decision delay is approximately 1.8 s. This delay is due to: delays of filters and structural elements, dealing with the detection pulses, and due to the worst expected

average pulse transit time. If adding the routine to seek for possible pacemaker patterns and the matching procedure, a learning period at the beginning of analysis is needed to accurately estimate the pattern of beat-by-beat intervals and to determine the match between the ECG and *P* signal annotation streams. The duration of such a learning procedure would also be dependent on the quality of the signals present.

There is certainly a room for further improvement of the detector. If processing ECG signals only, the current version of the detector leaves all detected heart beats in the noise intervals as they were detected. In the current version, the *P* signals are considered as equal candidates in the matching routine to be selected for the task of mapping their annotation streams into the final annotation stream. A routine that would gather heart beat positions detected in the simultaneous *P* signals of detection step I into a single *P* signal annotation stream can be devised. Such a routine would need to deal with different pulse transit times from different *P* signals. We did not devise a noise detection routine to assess the quality of the *P* signals. Furthermore, it would be useful to devise a post-processor of beat-to-beat intervals of the final annotation stream to check their validity in terms of erroneous intervals (invalid relative distances) and in terms of longer gaps. Such a post-processor would reject false positive detections, and would try to predict the positions of missing heart beats in longer gaps to set them accordingly.

Acknowledgments

This work was financed in part by the Slovenian Research Agency (ARRS) under the research project P3-0124—Metabolic and inborn factors of reproductive health, birth II. Result presented here are in the scope of PhD thesis that is being prepared by Urška Pangerc, University of Ljubljana, Faculty of Computer and Information Science.

References

Adnan M, Jiang Z and Choi S 2009 Development of QRS detection algorithm designed for wearable cardiorespiratory system *Comput. Methods Programs Biomed.* **93** 20–31

Behar J, Johnson A, Clifford G D and Oster J 2014 A comparison of single channel fetal ECG extraction methods *Ann. Biomed. Eng.* **42** 1340–53

Chen Y and Duan H 2005 A QRS Complex detection algorithm based on mathematical morphology and envelope *Proc. IEEE 27th Ann. Conf. Engineering in Medicine and Biology* (*Shanghai, China, 17–18 January 2006*) pp 4654–57

Clifford G D, Long W J, Moody G B and Szolovits P 2009 Robust parameter extraction for decision support using multimodal intensive care data *Phil. Trans. R. Soc.* A **367** 411–29

De Cooman T, Goovaerts G, Varon C, Widjaja D and Van Huffel S 2014b Heart beat detection in multimodal data using signal recognition and beat location estimation *Comput. Cardiol.* **41** 257–60 (www.cinc.org/archives/2014/pdf/0257.pdf)

Ding Q, Bai Y, Erol Y B, Salas-Boni R, Zhang X, Li L and Hu X 2014a Multimodal information fusion for robust heart beat detection *Comput. Cardiol.* **41** 261–64 (www.cinc.org/archives/2014/pdf/0261.pdf)

Ding J J, Huang C W, Ho YL, Hung C S, Lin Y H and Chen Y H 2014b An efficient selection, scoring, and variation ratio test algorithm for ECG R-wave peak detection *Exp. Clin. Cardiology* **20** 4256–63

Efron B 1979 Bootstrap methods: another look at the jackknife *Ann. Stat.* **7** 1–26

Elgendi M 2013 Fast QRS detection with an optimized knowledge-based method: evaluation on 11 standard ECG databases *PLoS ONE* **8** e73557

Elgendi M, Eskofier B, Dokos S and Abbot D 2014 Revisiting QRS detection methodologies for portable, wearable, battery-operated, and wireless ECG systems *PLoS One* **9** e84018

Ghaffari A, Golbayani H and Ghasemi M 2008 A new mathematical based QRS detector using continuous wavelet transform *Comput. Electr. Eng.* **34** 81–91
Ghosh S, Feng M, Nguyen H and Li J 2014 Predicting heart beats using co-occurring constrained sequential patterns *Comput. Cardiol.* **41** 265–68 (www.cinc.org/archives/2014/pdf/0265.pdf)
Gierałtowski J, Ciuchciński K, Grzegorczyk I, Kośna K, Soliński M and Podziemski P 2014 Algorithm for detection of heart rate from noisy, multimodal recordings *Comput. Cardiol.* **41** 253–56 (www.cinc.org/archives/2014/pdf/0253.pdf)
Gilián Z, Kovács P and Samiee K 2014 Rhythm-based accuracy improvement of heart beat detection algorithms *Comput. Cardiol.* **41** 269–72 (www.cinc.org/archives/2014/pdf/0269.pdf)
Goldberger A L, Amaral L A, Glass L, Hausdorff J M, Ivanov P C, Mark R G, Mietus J E, Moody G B, Peng C K and Stanley H E 2000 PhysioBank, PhysioToolkit, and PhysioNet: components of a new research resource for complex physiologic signals *Circulation* **101** e215–20
Gonzalez R C and Woods R E 2008 *Digital Image Processing* 3rd edn (Upper Saddle River, NJ: Prentice Hall)
Hamilton P S and Tompkins W J 1986 Quantitative Investigation of QRS detection rules using the MIT/BIH Arrhythmia database *IEEE Trans. Biomed. Eng.* **33** 1157–65
Ichimaru Y and Moody G B 1999 Development of the polysomnographic database on CD-ROM *Psychol. Clin. Neurosci.* **53** 175–77
Jager F, Taddei A, Moody G B, Emdin M, Antolič G, Dorn R, Smrdel A, Marchesi C and Mark R G 2003 Long-term ST database: a reference for the development and evaluation of automated ischaemia detectors and for the study of the dynamics of myocardial ischaemia *Med. Biol. Eng. Comput.* **41** 172–82
Johannesen L, Vicente J, Scully C G, Galeotti L and Strauss D G 2014 Robust algorithm to locate heart beats from multiple physiological waveforms *Proc. Computing in Cardiology Conf.* (*Boston*) pp 277–80
Johnson A E, Behar J, Andreotti F, Clifford G D and Oster J 2014 R-peak estimation using multimodal lead switching *Comput. Cardiol.* **41** 281–4 (www.cinc.org/archives/2014/pdf/0281.pdf)
Köhler BU, Henning C and Olgmeister R 2002 The principles of software QRS detection *IEEE Eng. Med. Biol.* **21** 42–57
Li C, Zheng C and Tai C 1995 Detection of ECG characteristic points using wavelet transforms *IEEE Trans. Biomed. Eng.* **42** 21–28
Lynn P A 1977 Online digital filter for biological signals: some fast designs for a small computer *Med. Biol. Eng. Comput.* **15** 534–40
Martínez JP, Almeida R, Olmos S, Rocha A P and Laguna P 2004 A wavelet-based ECG delineator: evaluation on standard databases *IEEE Trans. Biomed. Eng.* **51** 570–81
Moody G B, Feldman C L and Bailey J J 1993 Standards and applicable databases for long-term ECG monitoring *Electrocardiogram* **26** 151–5
Moody G B and Mark R G 2001 The impact of the MIT–BIH Arrhythmia database 2001 *IEEE Eng. Med. Biol.* **20** 45–50
Moody G B, Moody B and Silva I 2014 Robust detection of heart beats in multimodal data: the Physionet/Computing in Cardiology challenge *Comput.Cardiol.* **41** 549–52 (www.cinc.org/archives/2014/pdf/0549.pdf)
Oweis R J and Al-Tabbaa B O 2014 QRS detection and heart rate variability analysis: a survey *Biomed. Sci. Eng.* **2** 13–4
Pahlm O and Sörnmo L 1984 Software QRS detection in ambulatory monitoring: a review *Med. Biol. Eng. Comput.* **22** 289–97
Pangerc U and Jager F 2014 Robust detection of heart beats in multimodal data using integer multiplier digital filters and morphological algorithms *Comput. Cardiol.* **41** 285–88 (www.cinc.org/archives/2014/pdf/0285.pdf)
Pan J and Tompkins W J 1985 A real-time QRS detection algorithm *IEEE Trans. Biomed. Eng.* **32** 230–36
Physionet 2014a www.physionet.org/physiotools/wag/gqrs-1.htm
Physionet 2014b www.physionet.org/physiotools/wag/wabp-1.htm
Pimentel M A, Santos M D, Springer D B and Clifford G D 2014 Hidden semi-Markov model-based Heart beat detection using multimodal data and signal quality indices *Comput. Cardiol.* **41** 553–6 (www.cinc.org/archives/2014/pdf/0553.pdf)
Plešinger F, Jurco J, Jurak P and Halamek J 2014 Robust multichannel QRS detection *Comput.Cardiol.* **41** 557–60 (www.cinc.org/archives/2014/pdf/0557.pdf)

Romero L I *et al* 2005 Continuous wavelet transform modulus maxima analysis of the electrocardiogram: beat characterization and beat-to-beat measurement *Int. J. Wavelets, Multiresolution Inf. Process.* **3** 19–42

Schulte R, Krug J and Rose G 2014 Identification of a signal for an optimal heart beat detection in multimodal physiological datasets *Comput. Cardiol.* **41** 273–76 (www.cinc.org/archives/2014/pdf/0273.pdf)

Silva I, Moody B, Behar J, Johnson A, Oster J, Clifford G D and Moody G B 2015 Editorial: Robust detection of heart beats in multimodal data *Phys. Meas.* **36** 1629

Thakor N V, Webster J G and Tompkins W J 1984 Estimation of QRS complex power spectra for design of a QRS filter *IEEE Trans. Biomed. Eng.* **31** 702–06

Vollmer M 2014 Robust detection of heart beats using dynamic thresholds and moving windows *Comput. Cardiol.* **41** 569–72 (www.cinc.org/archives/2014/pdf/0569.pdf)

Yang B, Teo S K, Hoeben B, Monterola C and Su Y 2014 Robust identification of heart beats with blood pressure signals and noise detection *Comput. Cardiol.* **41** 565–8 (www.cinc.org/archives/2014/pdf/0565.pdf)

Yu J, Jeon T and Jeon M 2014 Heart beat detection method with estimation of regular intervals between ECG and blood pressure *Comput. Cardiol.* **41** 561–4 (www.cinc.org/archives/2014/pdf/0561.pdf)

Welch J P, Ford P J, Teplick R S and Rubsamen R M 1991 The Massachusetts General Hospital-Marquette Foundation Hemodynamic and Electrocardiographic database—comprehensive collection of critical care waveforms *Clin. Monit.* **7** 96–7

Zhang F and Lian Y 2009 QRS detection based on multiscale mathematical morphology for wearable ECG devices in body area networks *IEEE Trans. Biomed. Circuits Syst.* **3** 220–28

Zong W, Heldt T, Moody G B and Mark R G 2003 An open-source algorithm to detect onset of arterial blood pressure *Proc. Computing in Cardiology Conf.* (*Thessaloniki*) pp 259–62